CERN
CH1211 Geneva 23
Switzerland

Engineering Department

EDMS NO.	REV.	VALIDITY
		In Work

REFERENCE
EN/CV

Date: 2019-05-16

TECHNICAL REPORT

CFD Studies on the Temperature Distribution

CLIC Main Tunnel – Drive Beam Machine

DOCUMENT PREPARED BY:	DOCUMENT CHECKED BY:	DOCUMENT APPROVED BY:
PEDRO CABRAL (EN-CV)		

Contents

HISTORY OF CHANGES

Reports	DATE	DESCRIPTION OF THE REPORT
Short Tunnel	16-05-2019	89,3 Tunnel
Long Tunnel	27-05-2019	156,3m Tunnel
Inverted Inlets and Outlets	28-05-2019	Inlets and outlets inverted & tunnel with 89,3m
Symmetric	04-06-2019	Inlets and outlets set so that the tunnel is symmetrical & 111,6m tunnel

1. INTRODUCTION

1. The CLIC beam alignment system requires a certain temperature stability in both space and time.
2. The HVAC basic design was done throughout 2018 and the resultant temperature distribution has to be consistent with the constraints posed by the alignment system.
3. The spatial temperature distribution during a steady state run mode is computed and reported to the CLIC team for evaluation.
4. Transient simulations will likely be done in the future.

2. GEOMETRY

AHUs are installed in the various technical alcoves to ensure the air conditioning of the main tunnel. Supply and extraction ducts are set along the tunnel, as shown in figure 1.

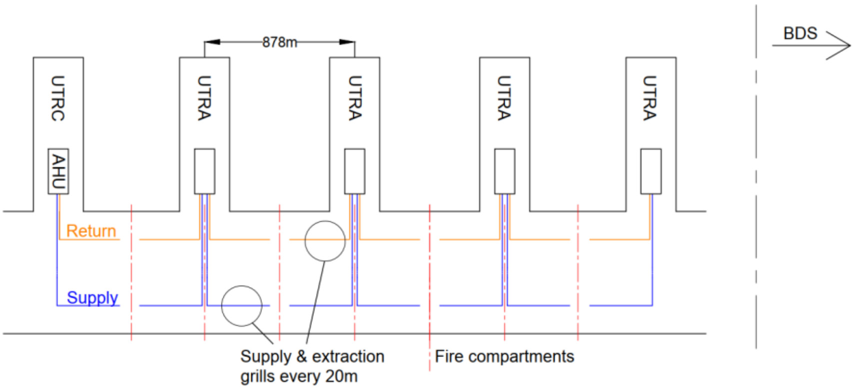

Figure 1. Tunnel cross section

Conditioned air is supplied through supply ducts and grilles. It is then extracted through extraction grilles and ducts to the respective air handling unit.

The tunnel cross section is presented in figure 2, where one can see the supply and extraction ducts, as well as the integration with the remaining services and utilities.

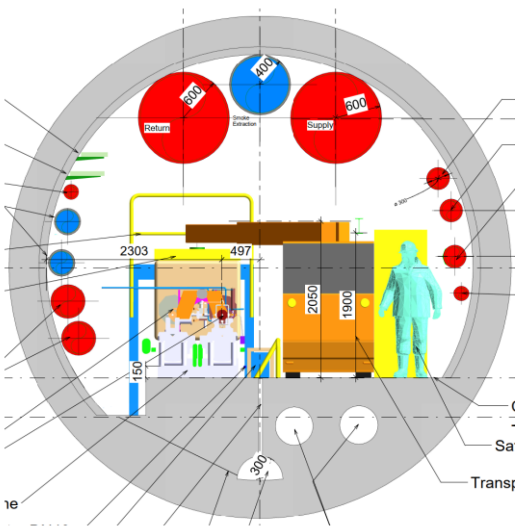

Figure 2. Tunnel cross section

3. NUMERICAL DOMAIN

The tunnel is long and contains a large number of geometrical complexities. A very demanding computational effort would have to be done in order to simulate the entire domain and all its particularities. Hence, the geometry was simplified to allow for expeditious simulations. Simultaneously, an effort was made to avoid oversimplifications and the consequent loss of realism.

The simplified cross section is presented in figure 3. The studied region and its setting in the overall geometry is shown in figure 4. The geometrical model is represented in figure 5.

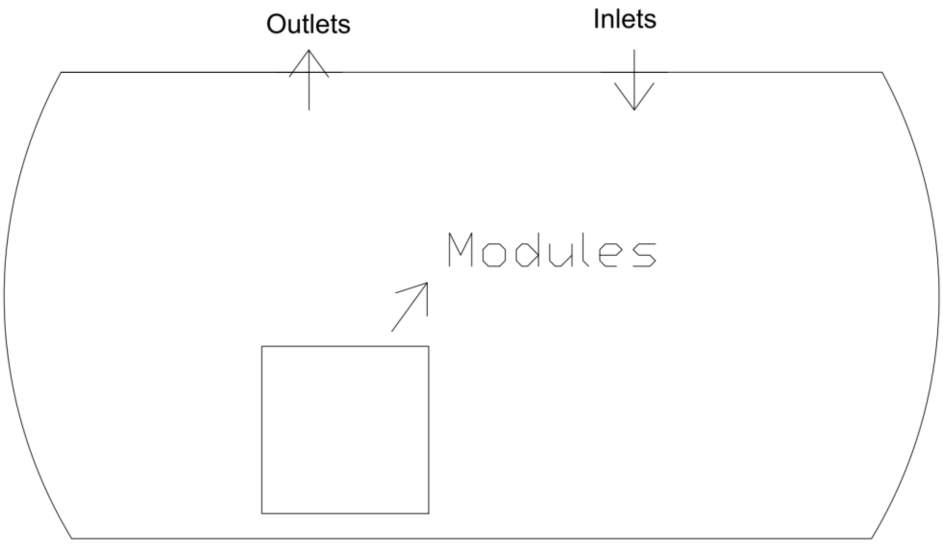

Figure 3. Simplified tunnel cross section

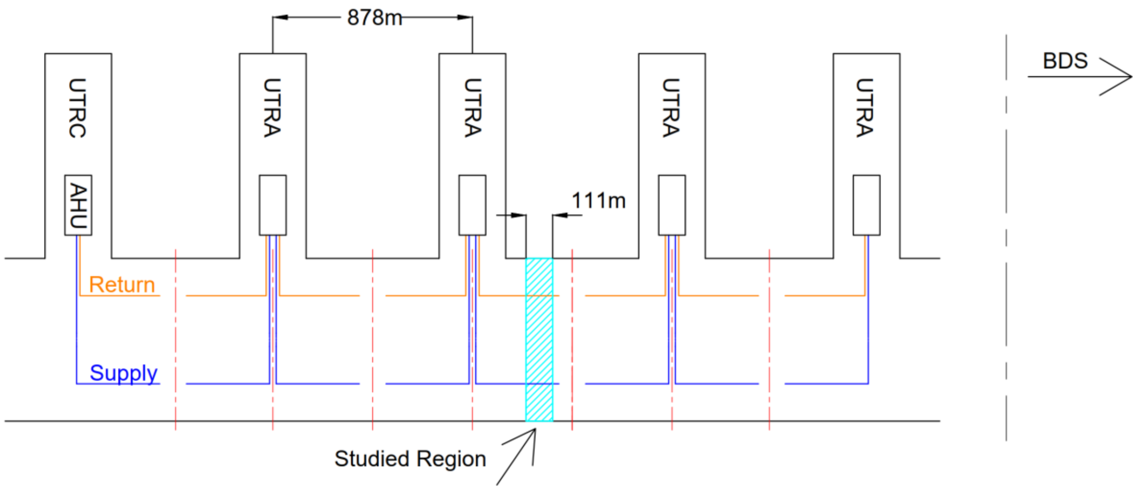

Figure 4. Studied region

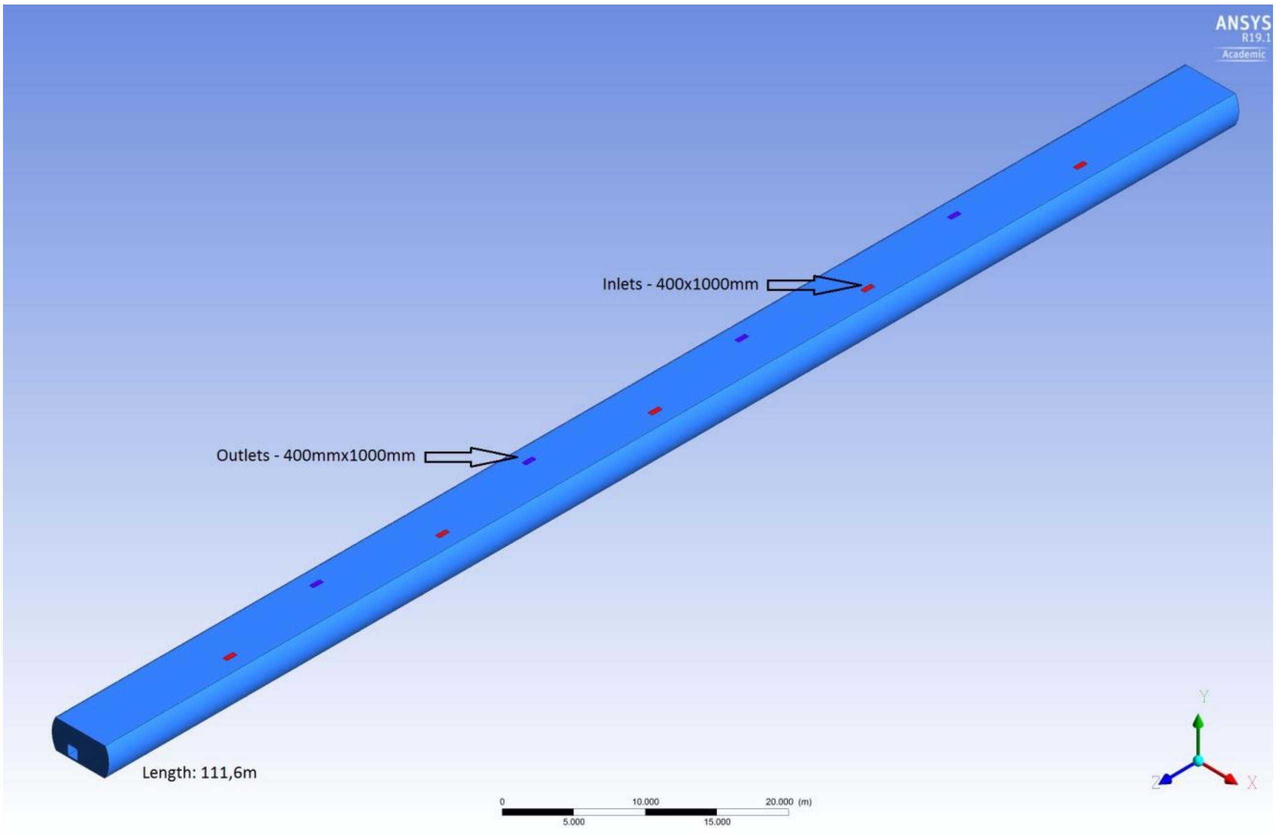

Figure 5. Complete numerical domain

4. MESH

The mesh has approximately 3,5 million elements. These have a tetrahedral geometry. The typical element size is 0,12m but further refinement is taken around the modules, the inlets and outlets as greater gradients are expected in these regions. The mesh element size close to these surfaces is set to 0,08m and the growth rate to 1,2. The mesh is shown in figures 6 and 7.

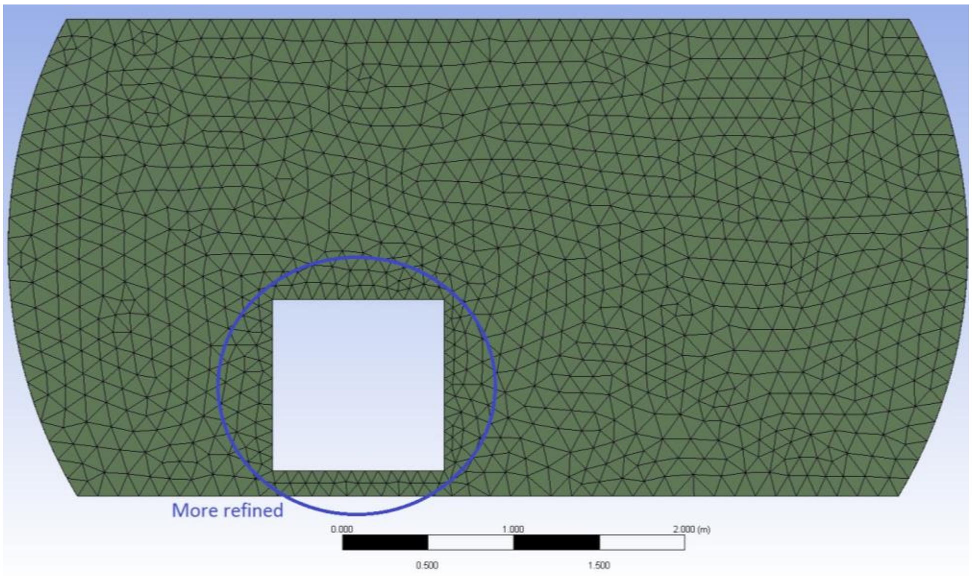

Figure 6. Cross section view of the mesh

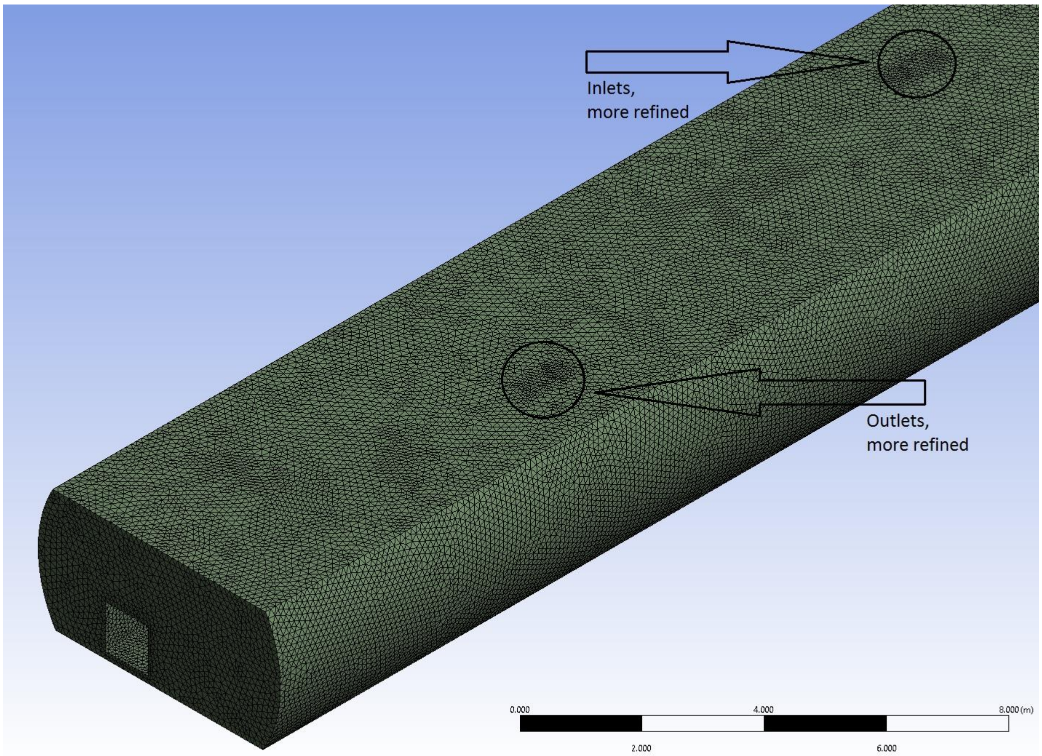

Figure 7. Inlet and outlet refinement

5. BOUNDARY CONDITIONS

1. Inlets – uniform 27 m/s velocity profile @ 23°C
2. Outlets – uniform zero relative pressure
3. Vertical and the top horizontal faces of the modules – heat source 98,4W/m^2

4. Walls, including the two limiting planes x0y and the modules – no slip and impermeability

The boundary conditions previously mentioned are represented in figures 8 and 9.

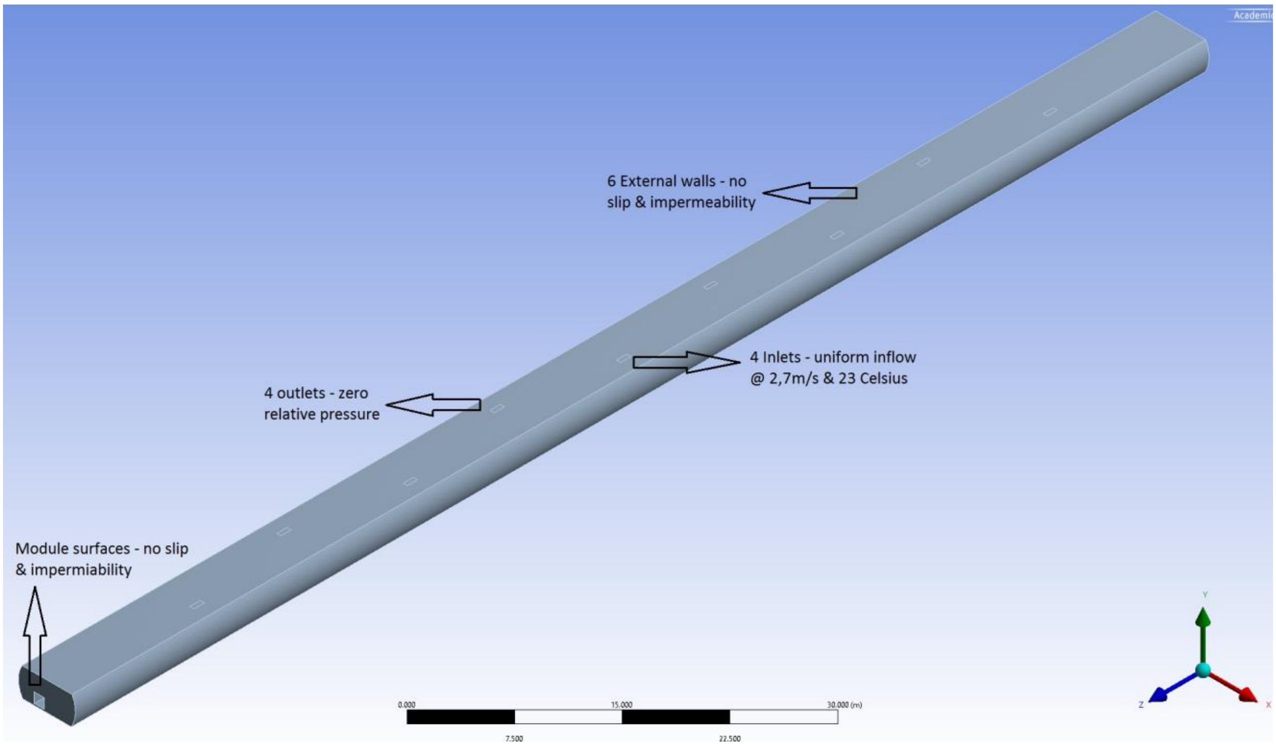

Figure 8. Inlet, outlet and wall boundary conditions

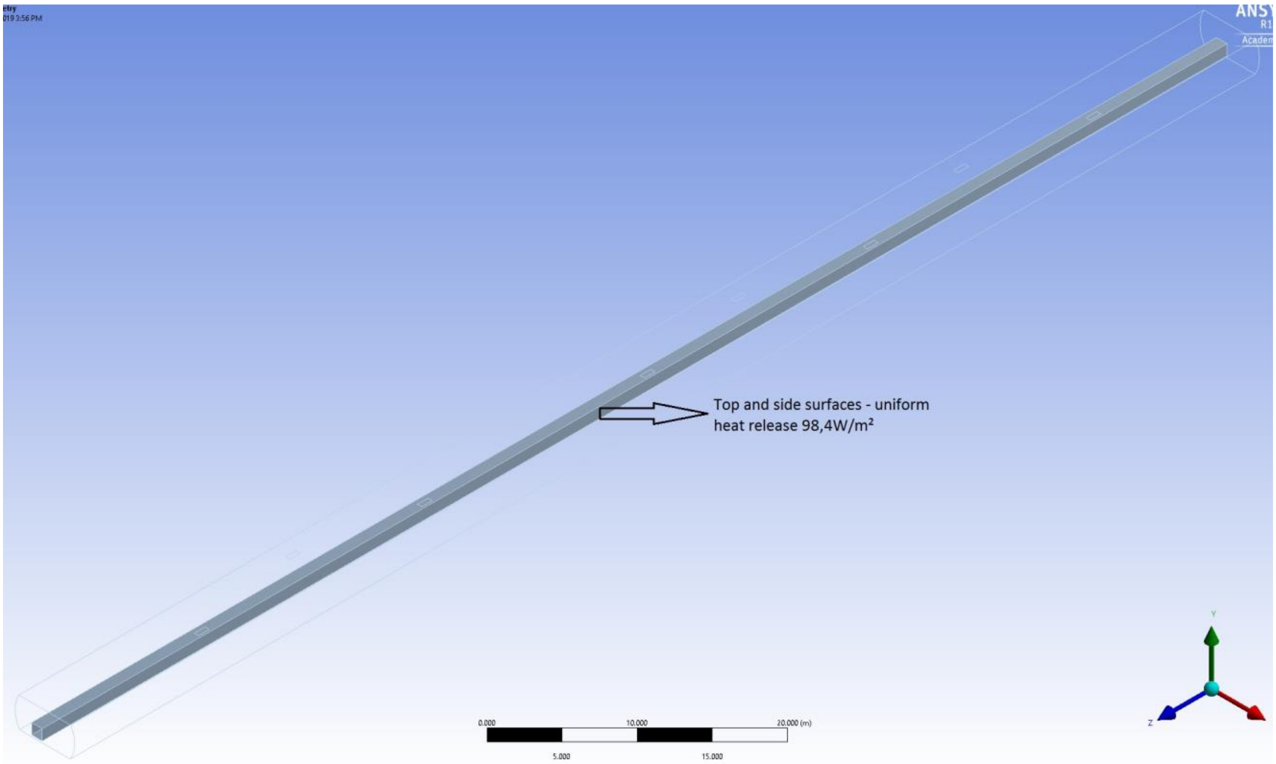

Figure 9. Heat source boundary condition

6. SIMULATION SET UP

a. Models – Steady state, k-ε realizable with scalable wall functions; energy equation is solved

b. Materials – incompressible ideal gas model

c. Methods

   i. Scheme – SIMPLE

   ii. Gradient – Least Squares Cell Based

   iii. Pressure – Second Order

   iv. Momentum – Second Order Upwind

   v. Turbulent Kinetic Energy – First Order Upwind

   vi. Turbulent Dissipation Rate –First Order Upwind

   vii. Energy – Second Order Upwind

d. Under-Relaxation Factors

   i. Pressure – 0,2

   ii. Density – 0,9

   iii. Body Forces – 1

   iv. Momentum – 0,5

   v. Turbulent Kinetic Energy – 0,5

   vi. Turbulent Dissipation Rate – 0,5

   vii. Turbulent Viscosity - 1

   viii. Energy – 0,9

7. CONVERGENCE

The residuals are controlled throughout the iteration process (figure 10), as well as some quantities of interest – the global mass (figure 11) and energy (figure 12) balances, the average temperature of the three heat releasing surfaces of the modules (figure 13), the average pressure at the inlets (figure 14) and the ambient temperature (figure 15).

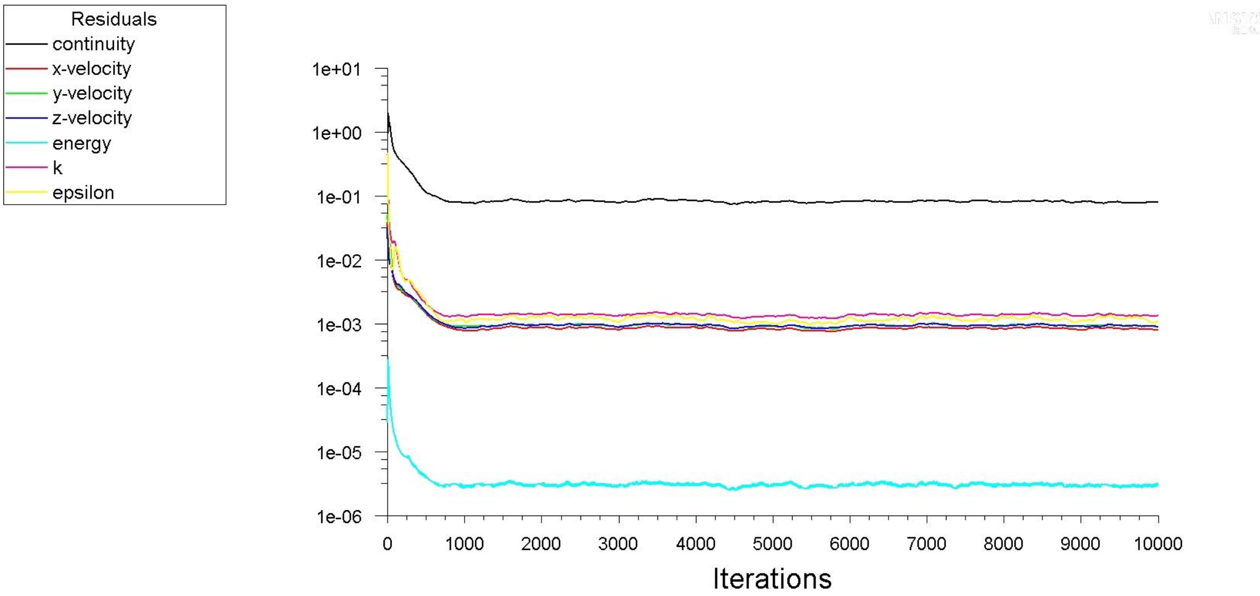

Figure 10. Residuals as a function of the iteration

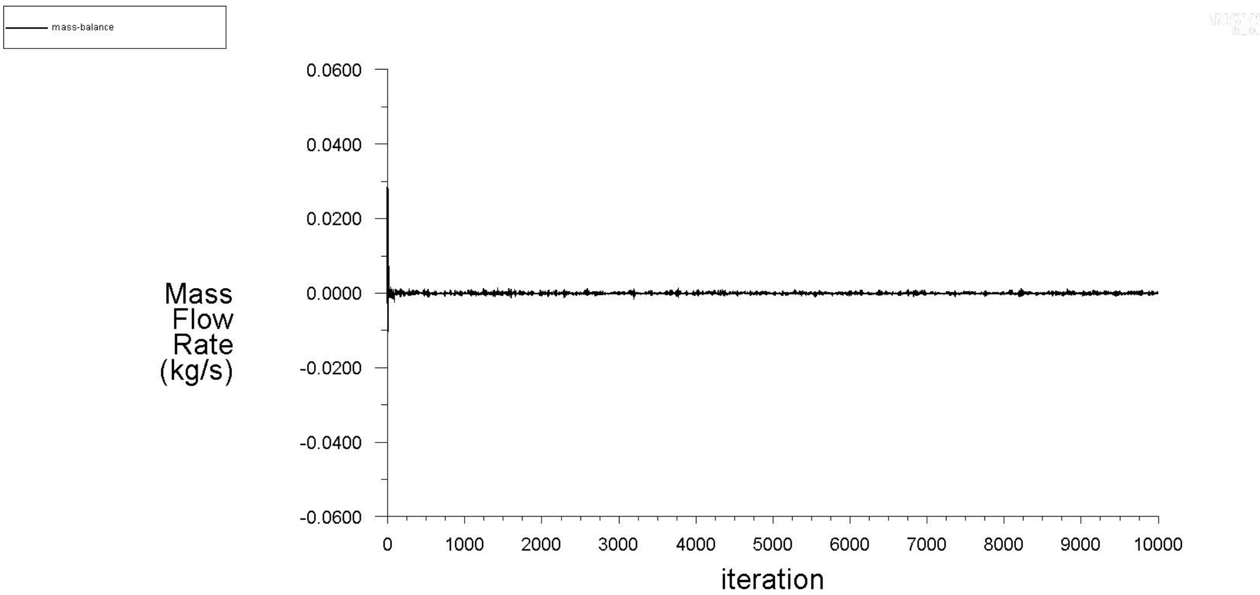

Figure 11. Overall mass balance as a function of the iteration

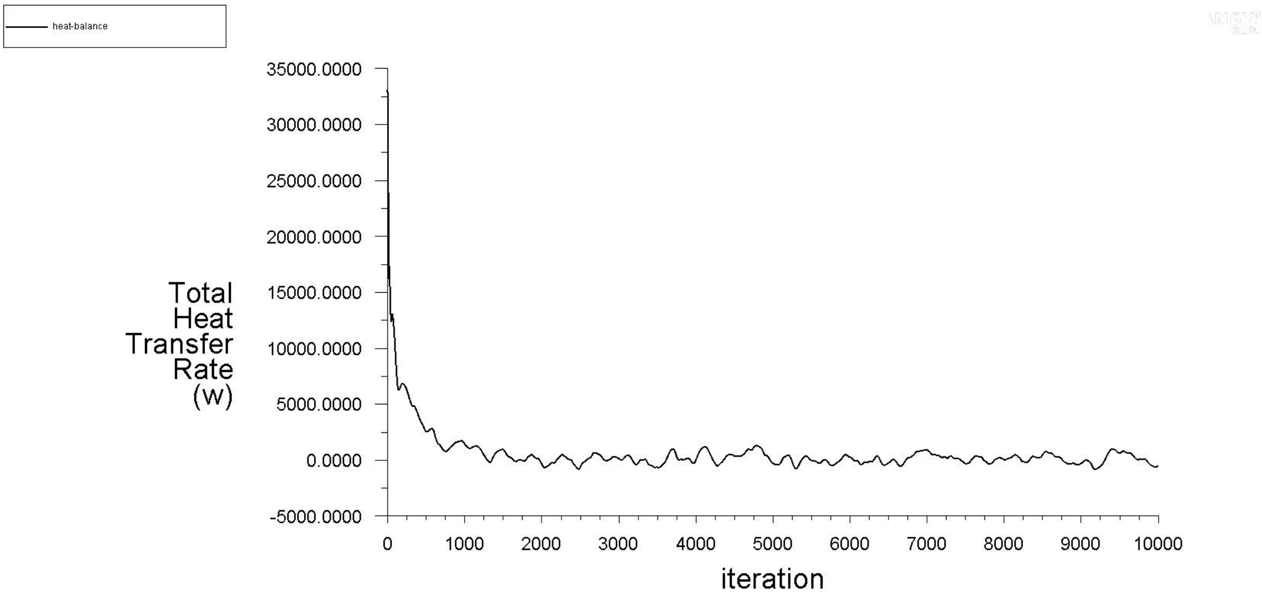

Figure 12. Overall energy balance as a function of the iteration

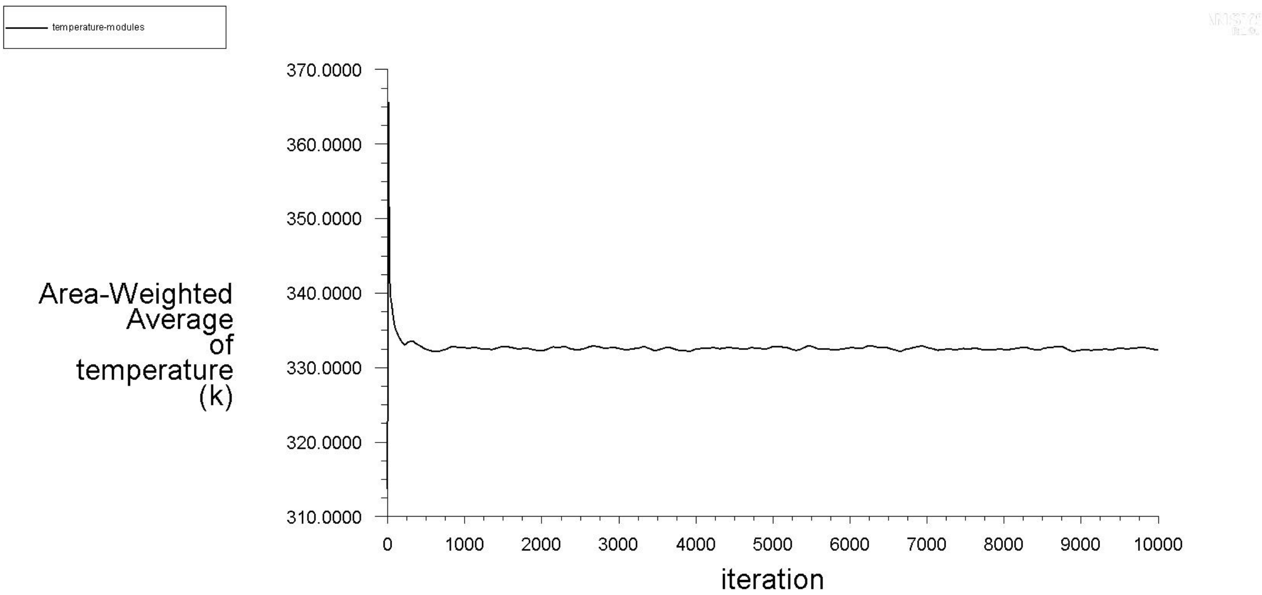

Figure 13. Average temperature of the three heat releasing surfaces of the modules as a function of the iteration

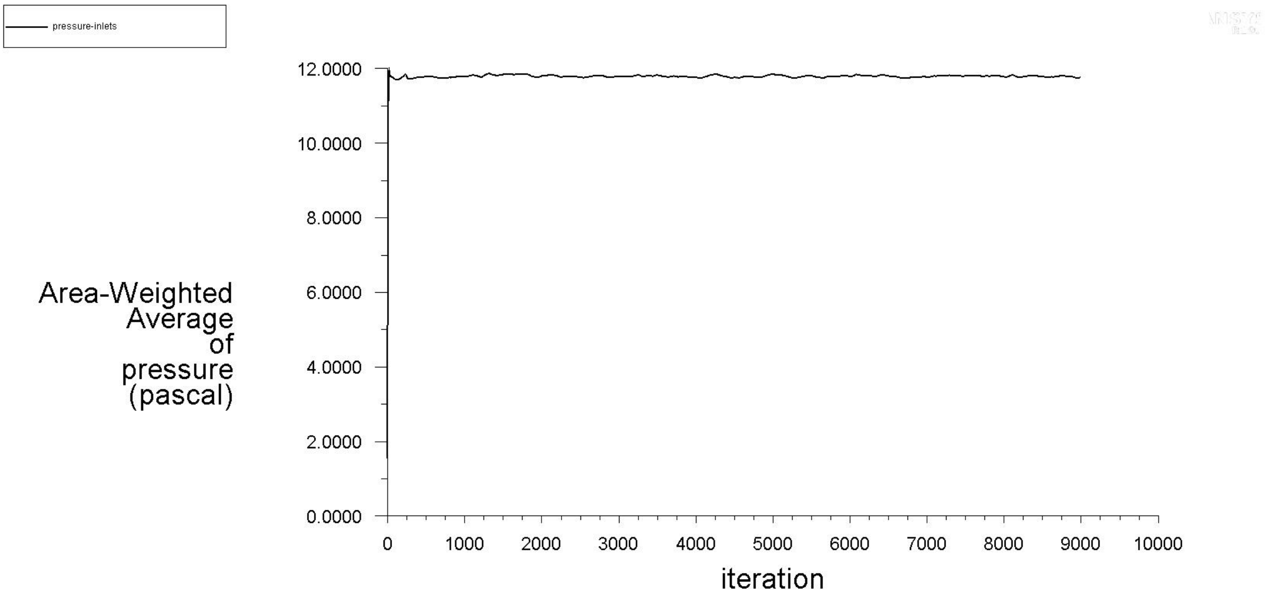

Figure 14. Average pressure at the inlets as a function of the iteration

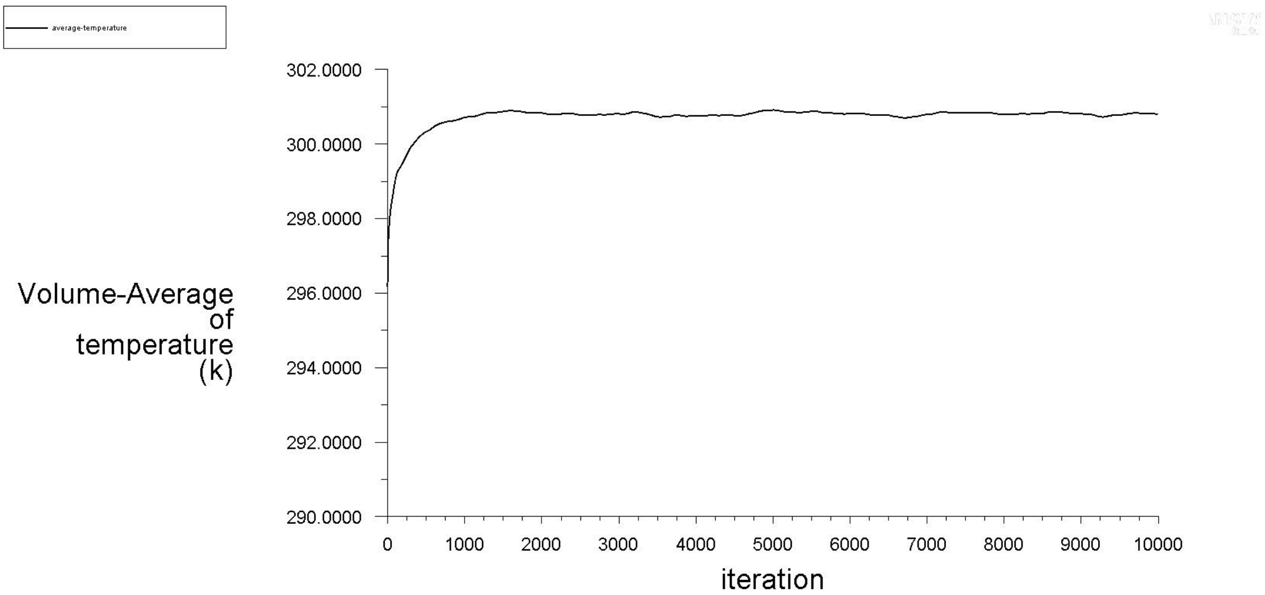

Figure 15. Ambient temperature as a function of the iteration

8. RESULTS

The temperature distribution was computed in 5 different transversal planes, placed between the central inlet and the central outlet, as represented in figure 16.

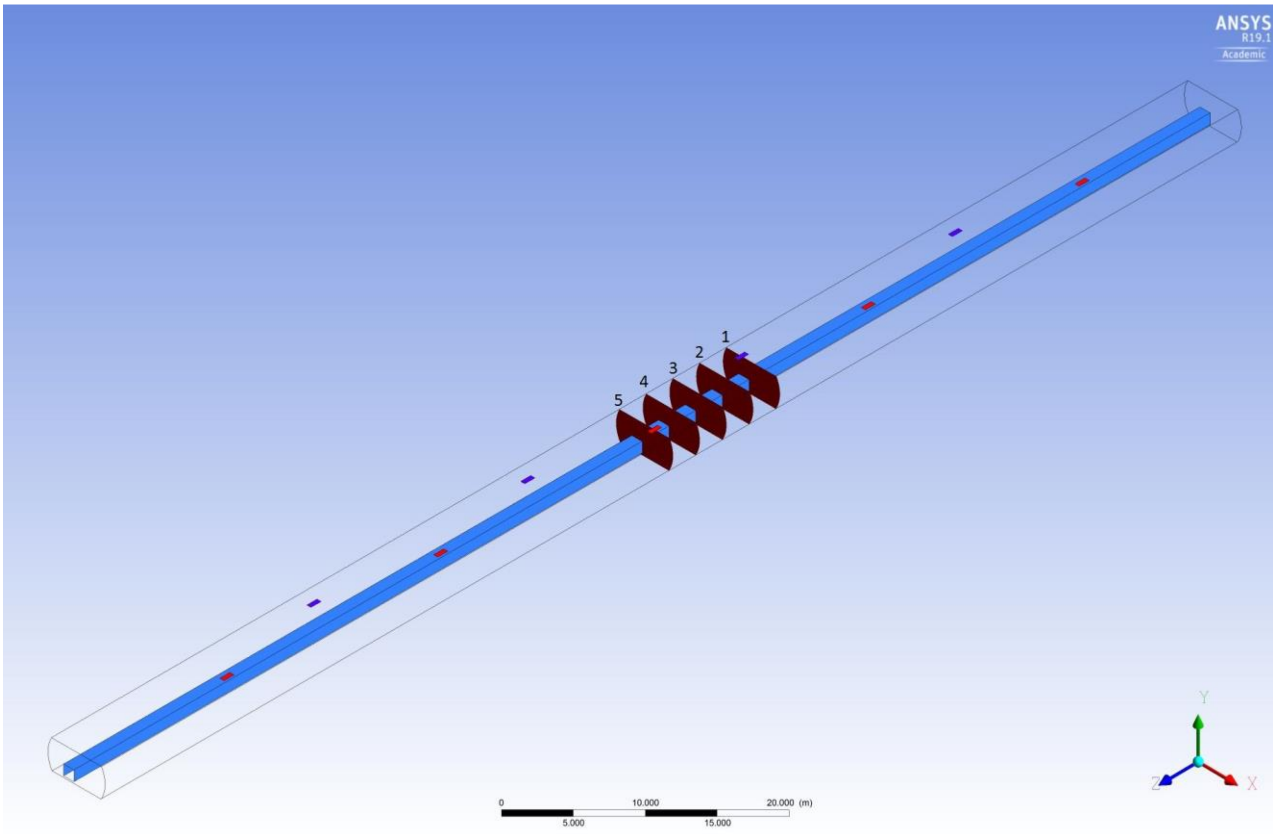

Figure 16. Transversal planes to compute the temperature distribution

The temperature distributions are presented bellow (figures 17 - 21). The temperature scale isn't set to study the region near the heat dissipating walls of the modules. The temperature in that region is higher than the maximum displayed by the scale. The scale is defined to study the regions relatively distanced from the modules. The temperatures in the wall of the modules are studied afterwards.

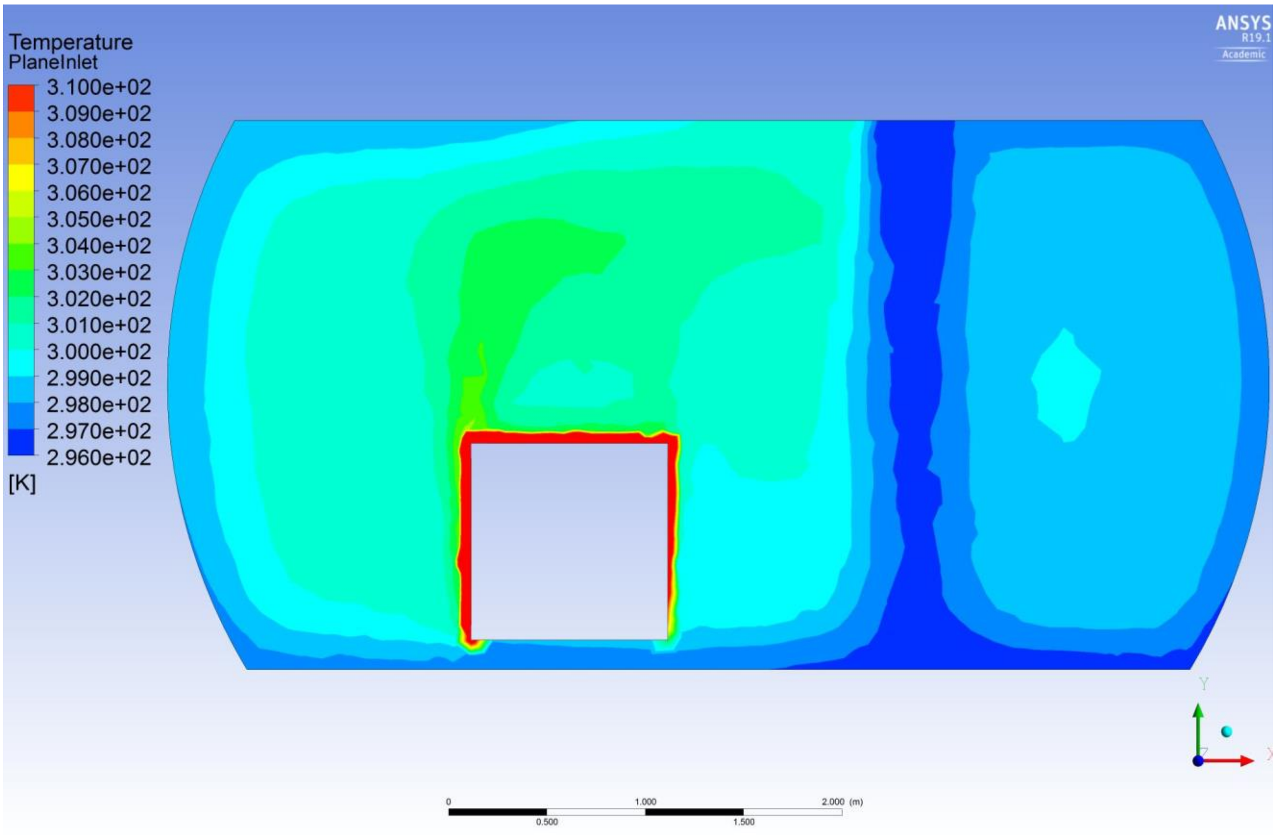

Figure 17. Temperature distribution in plane 1

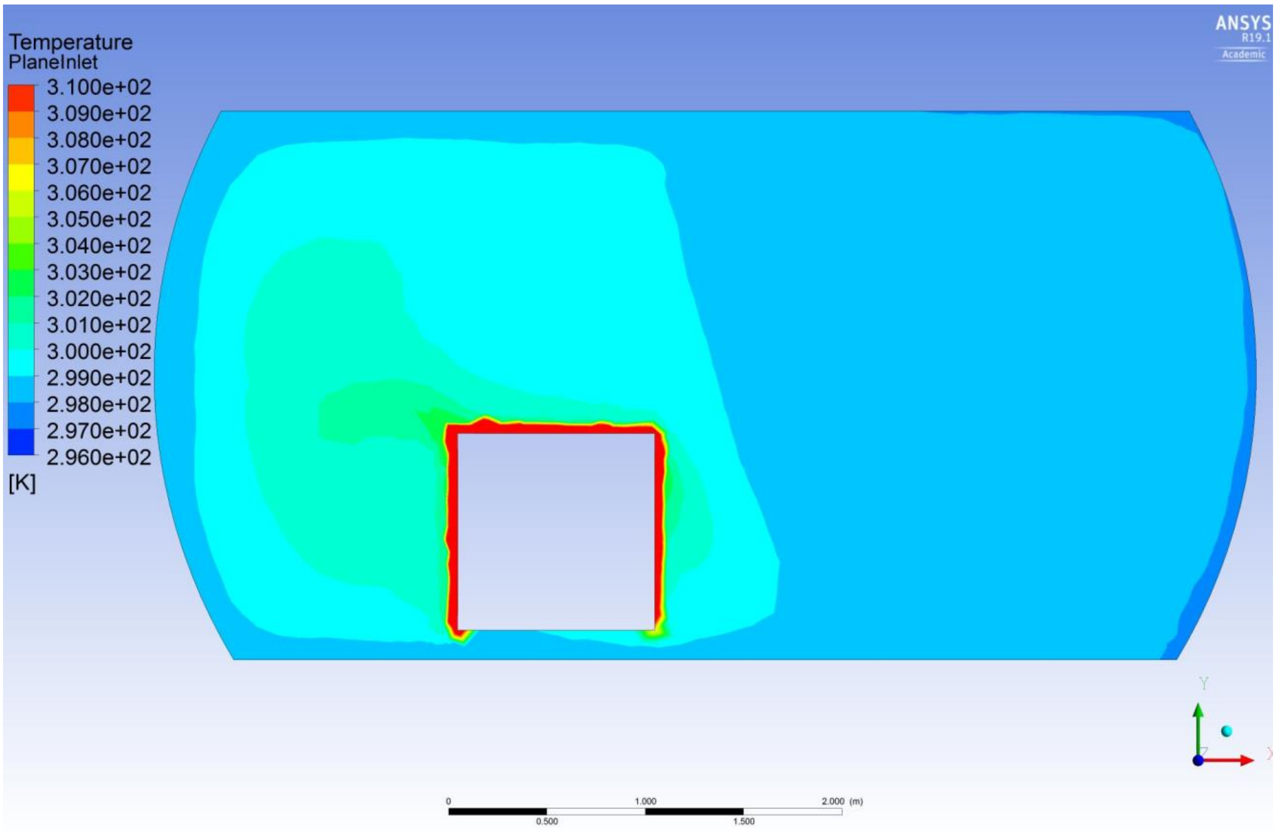

Figure 18. Temperature distribution in plane 2

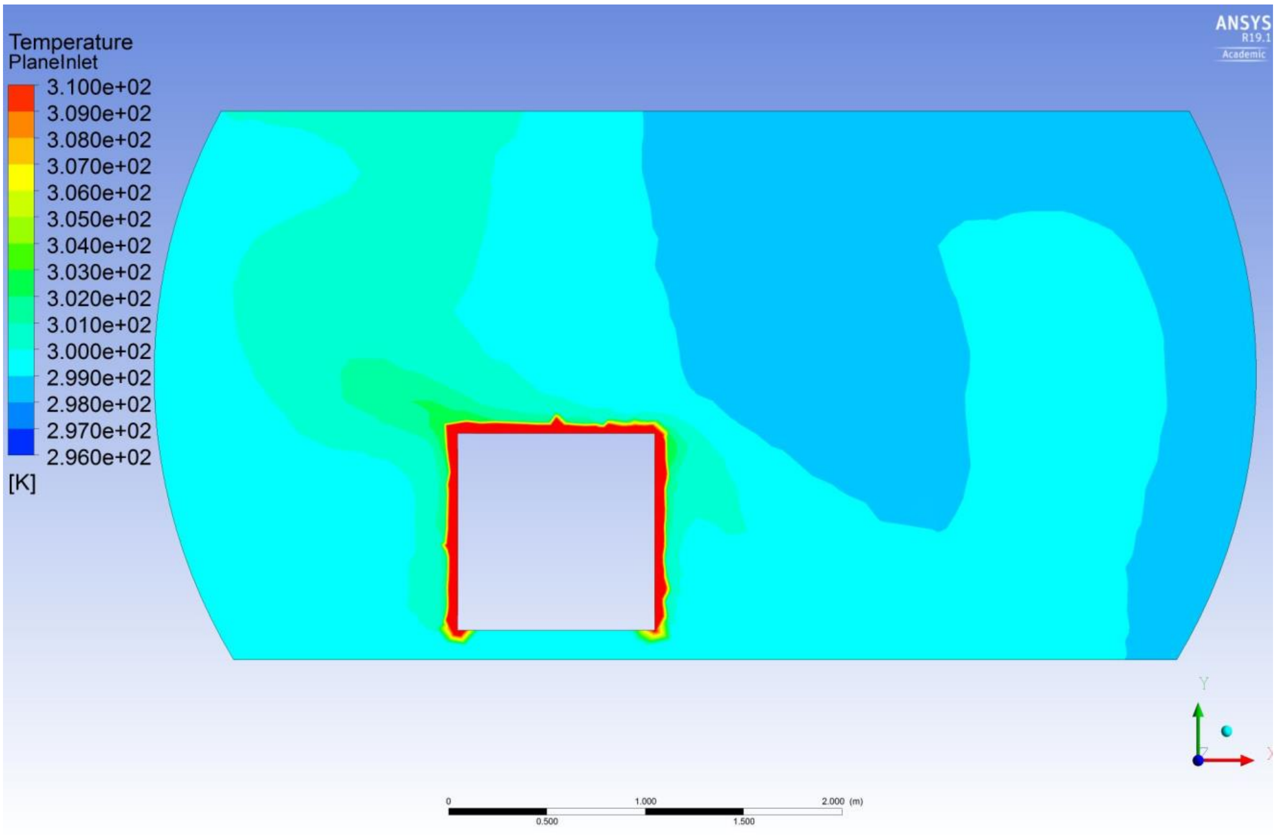

Figure 19. Temperature distribution in plane 3

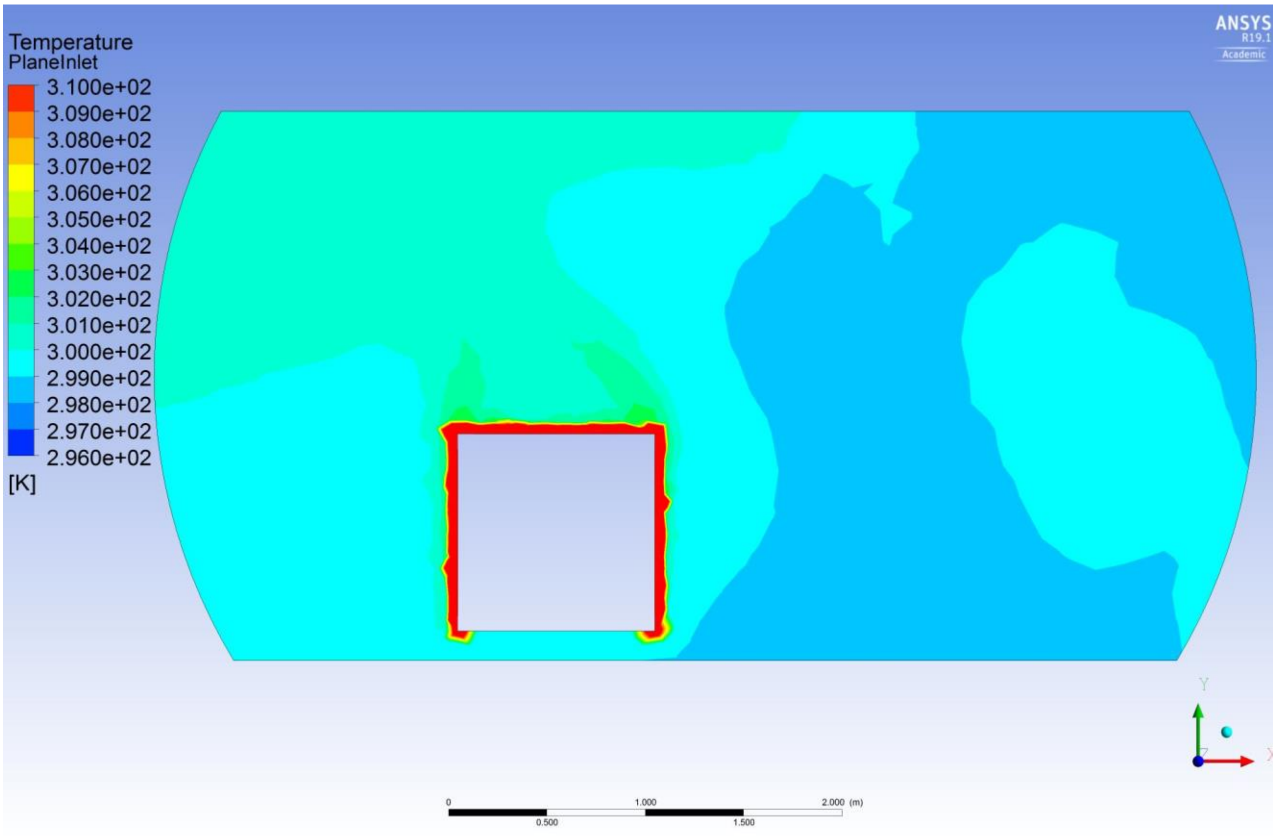

Figure 20. Temperature distribution in plane 4

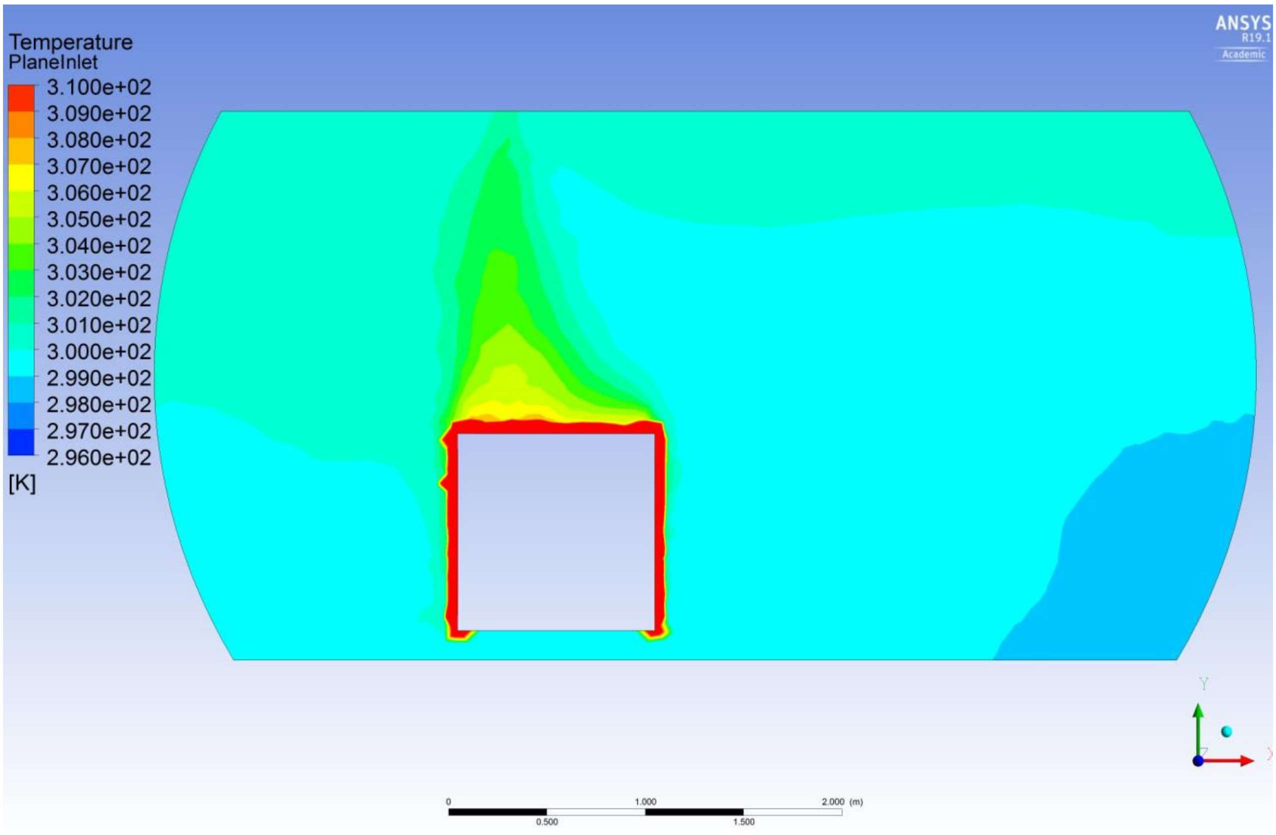

Figure 21. Temperature distribution in plane 5

The temperature distributions for the three heat emitting surfaces are presented below, as well as a schematic of the geometry (figures 22 – 26). The temperature scales are different from one figure to the next to allow the proper reading of the graphs.

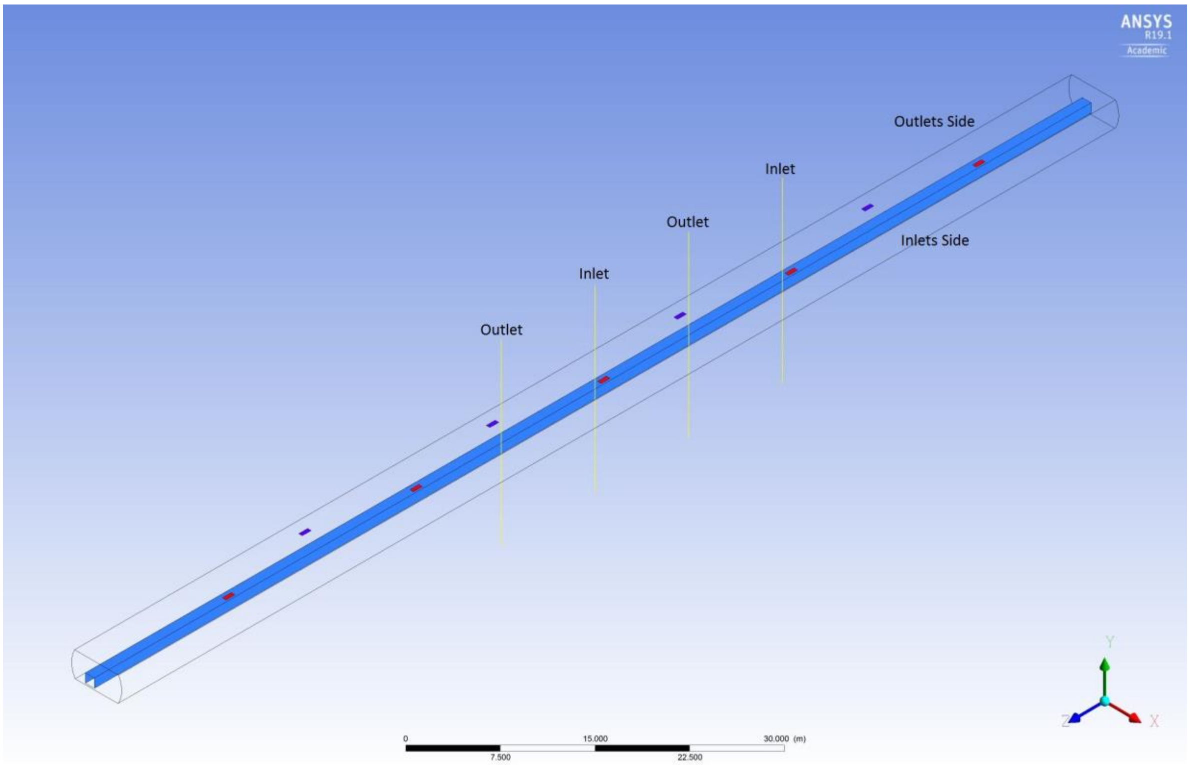

Figure 22. Schematic of the geometry and naming for the studied surfaces

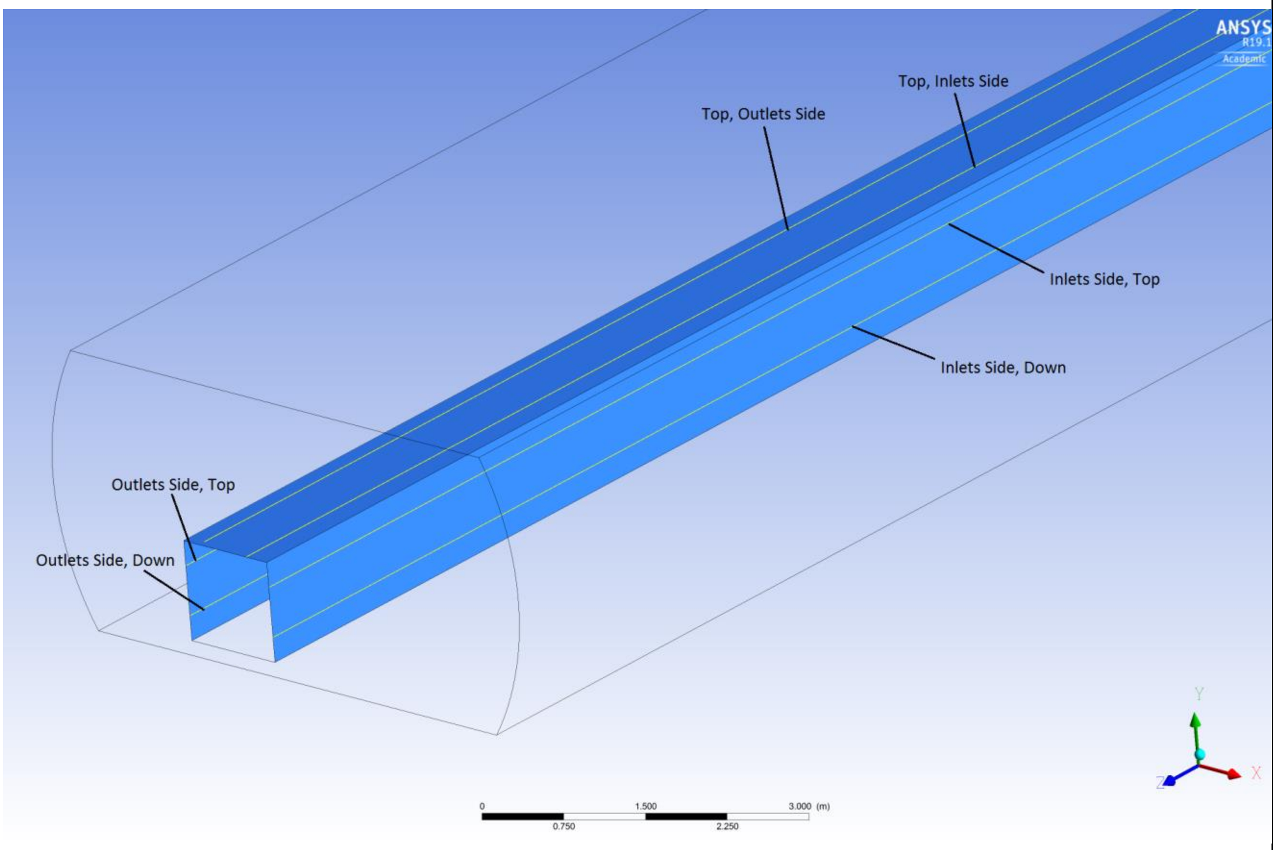

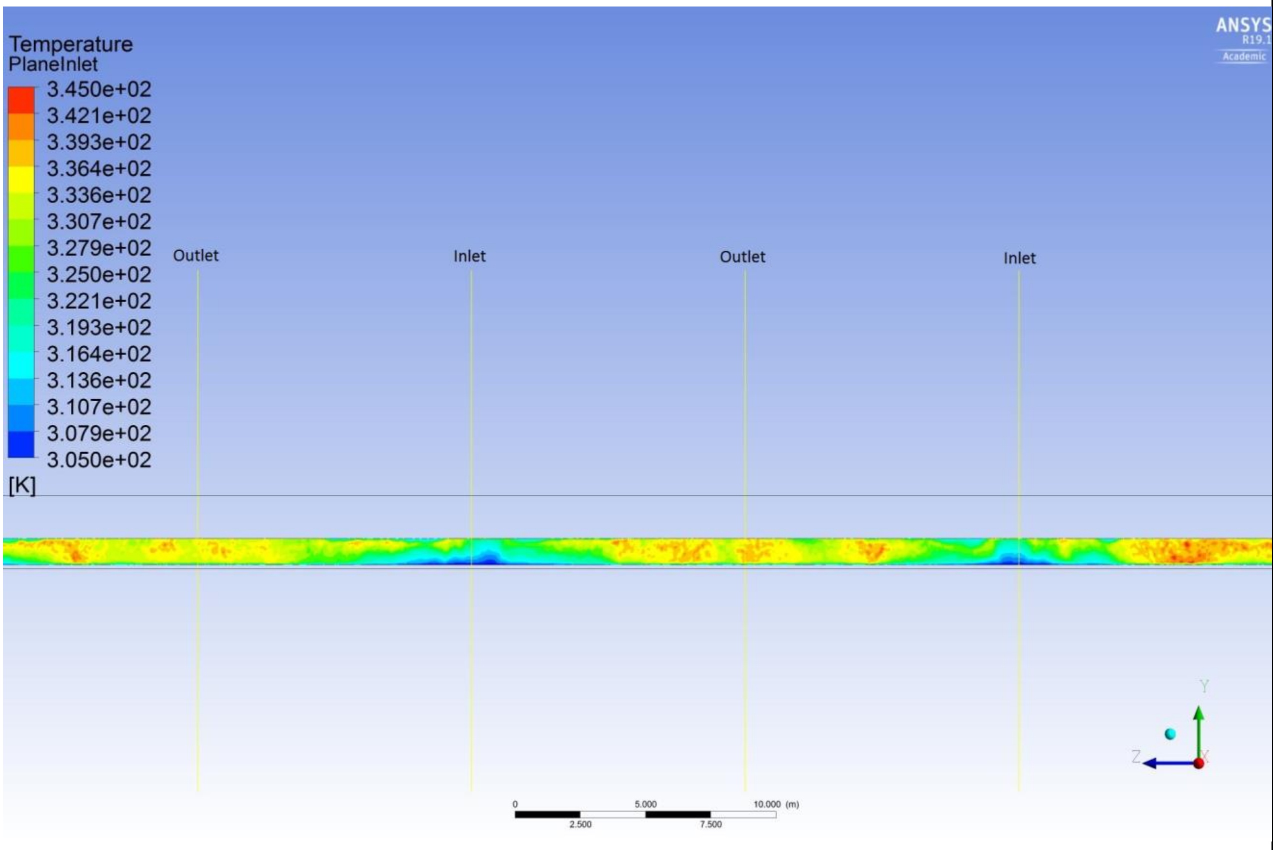

Figure 23. Temperature distribution in the vertical modules surface at the inlets side

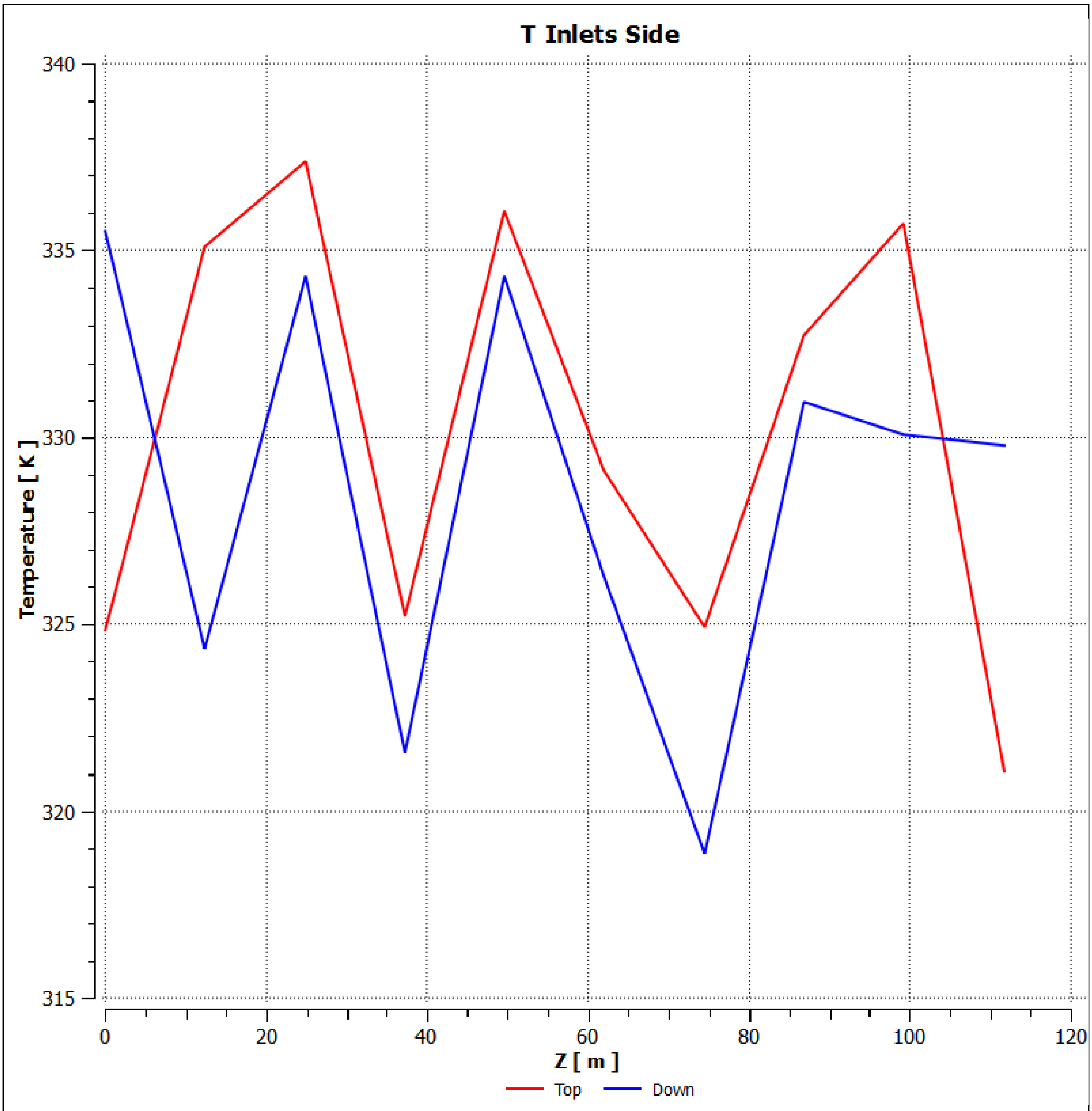
T Inlets Side
340
335
330
325
320
315
Temperature [K]
0
20
40
60
80
100
120
Z [m]
Top
Down

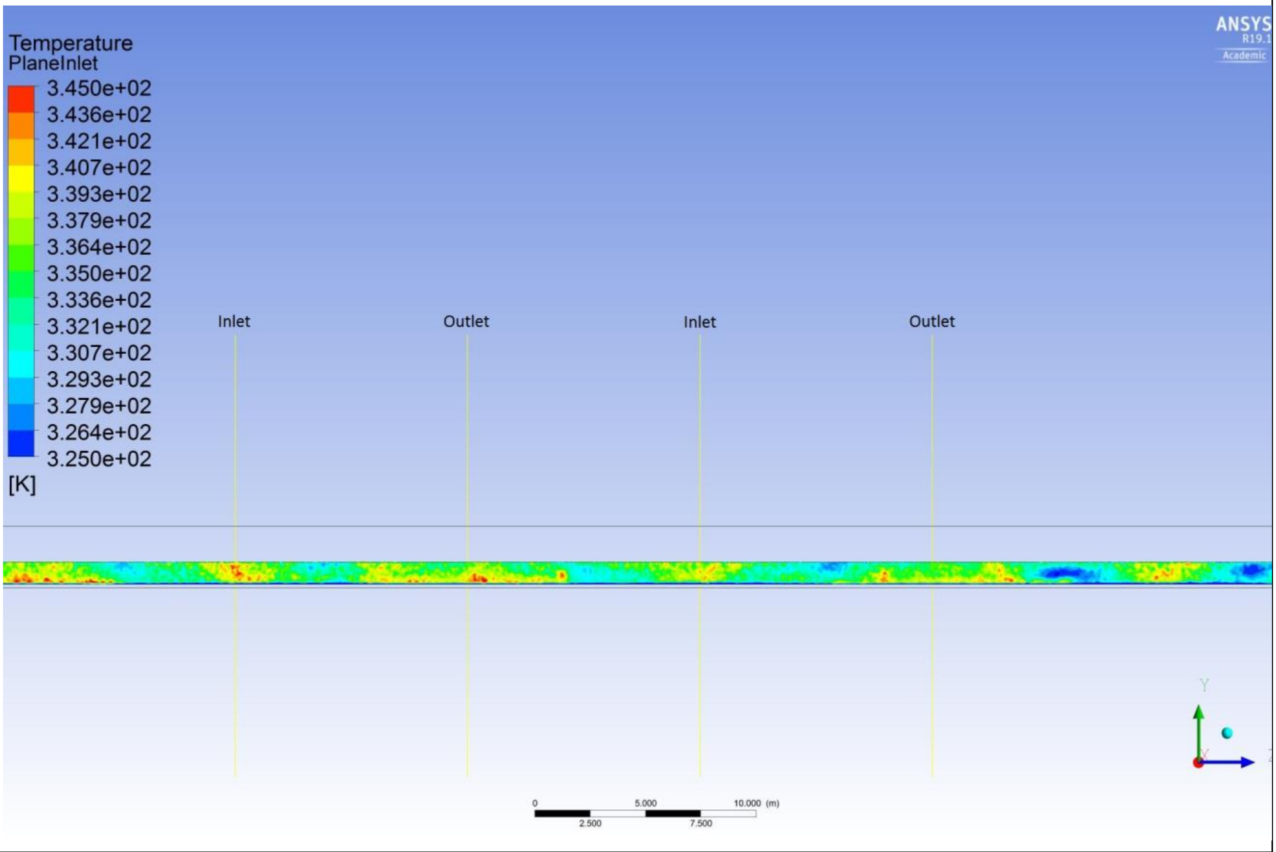

Figure 23. Temperature distribution in the vertical modules surface at the outlets side

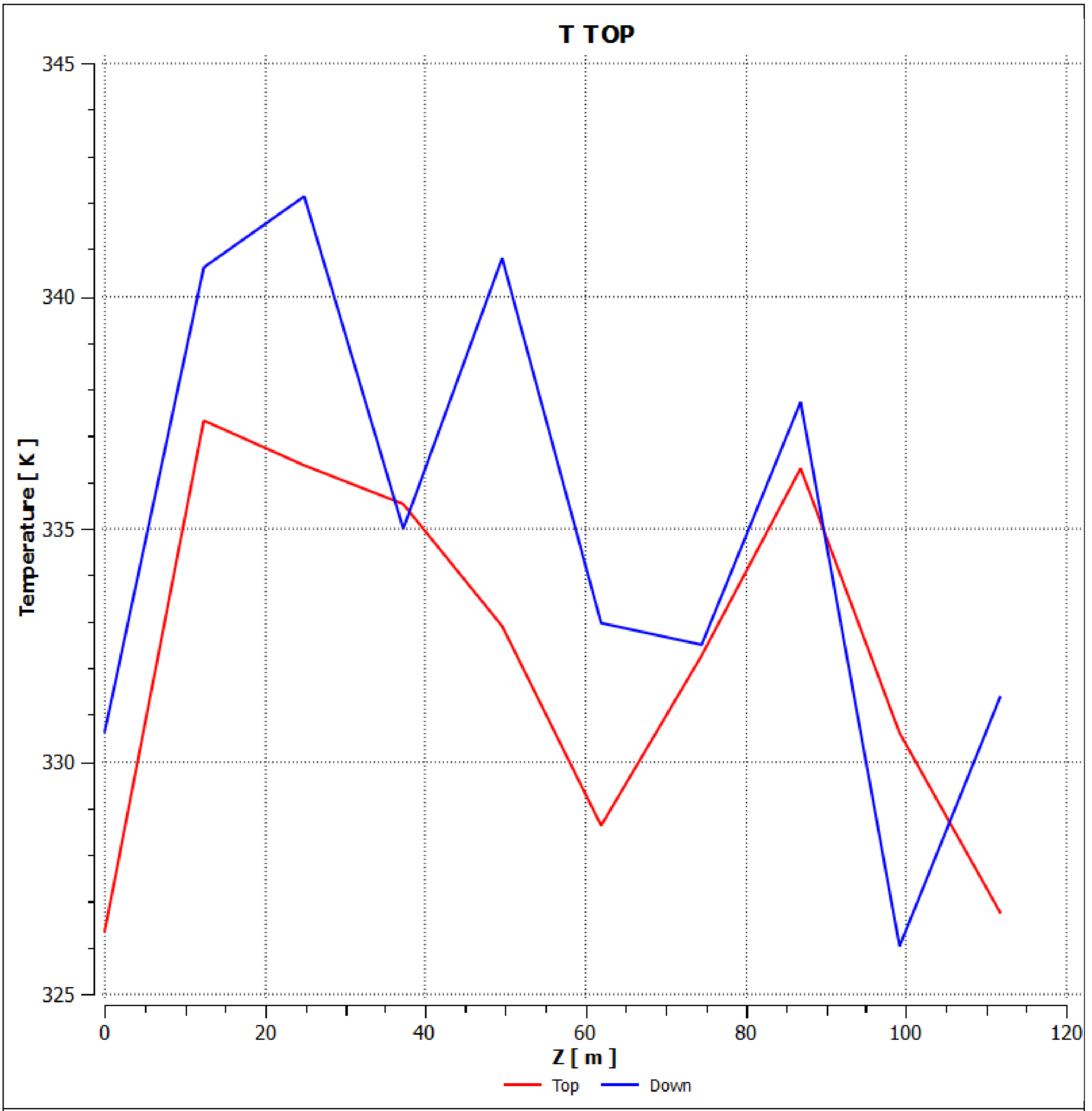
T TOP
Temperature [K]
345
340
335
330
325
0
20
40
60
80
100
120
Z [m]
Top
Down

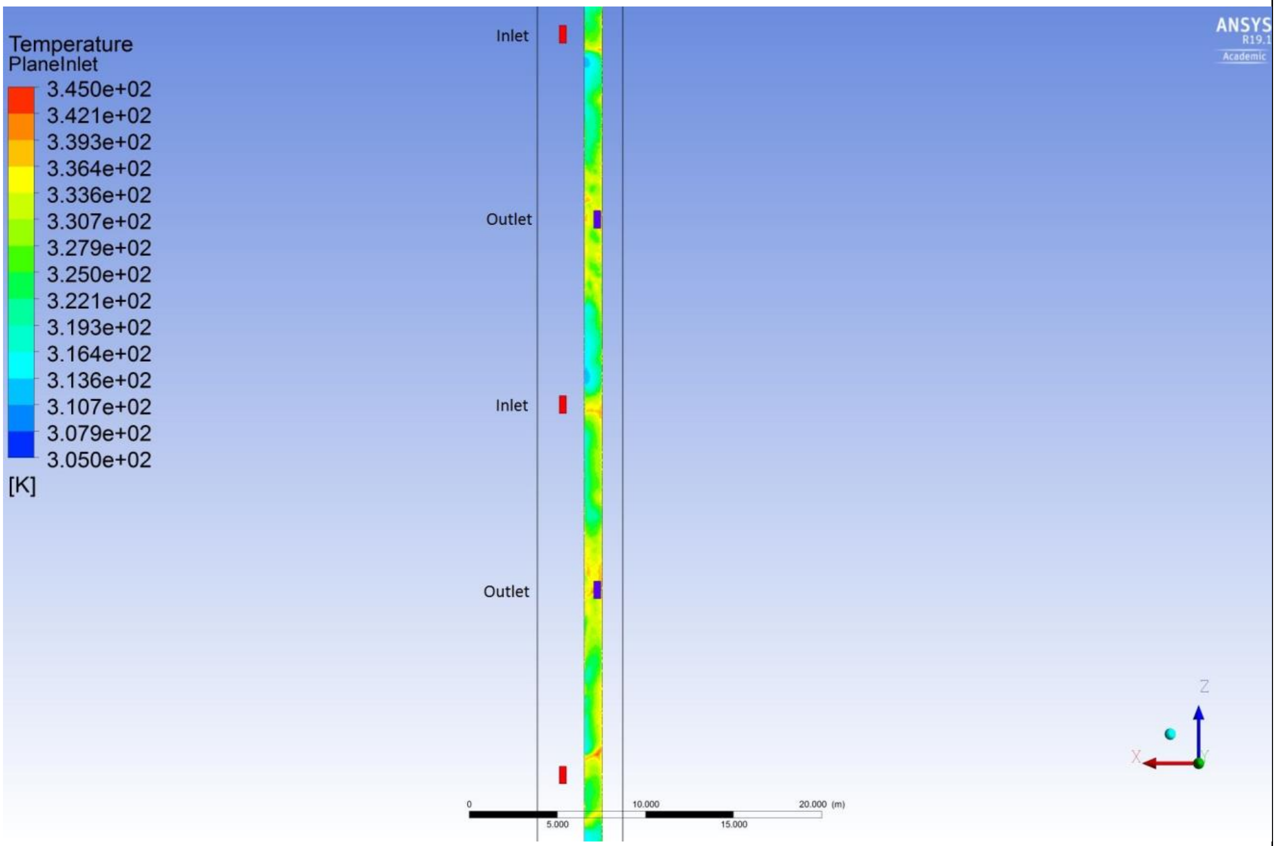

Figure 24. Temperature distribution in the top modules surface

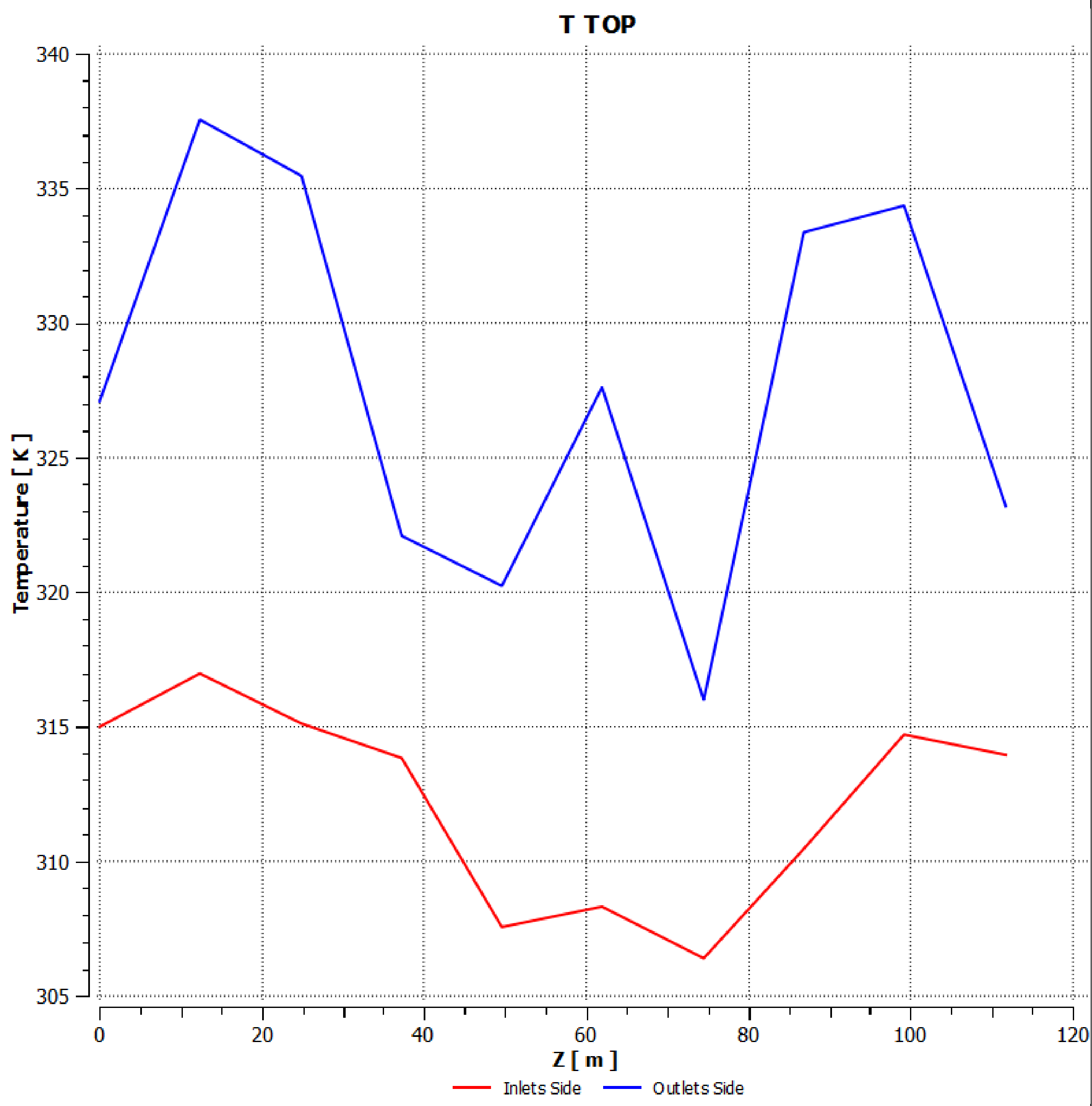

T TOP
340
335
330
325
320
315
310
305
Temperature [K]
0
20
40
60
80
100
120
Z [m]
Inlets Side
Outlets Side

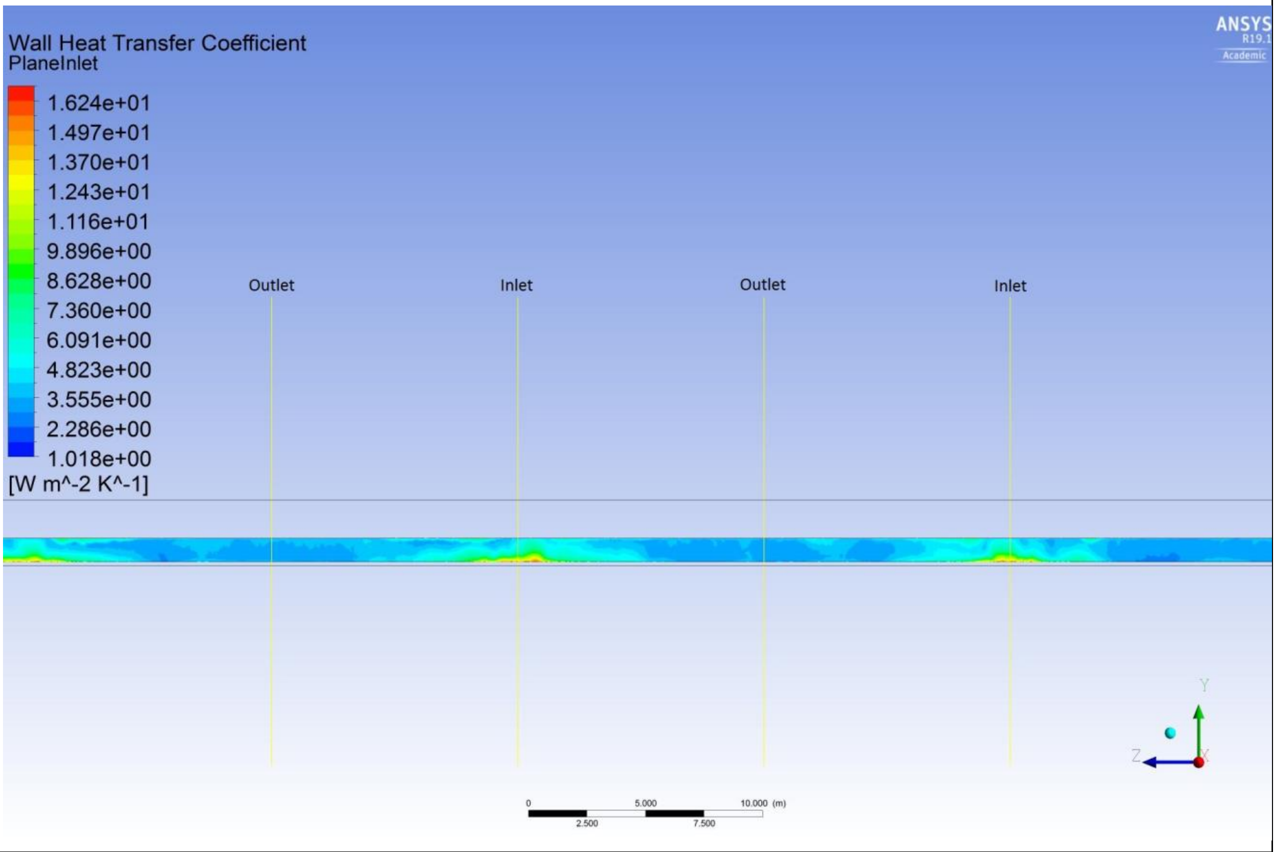
Wall Heat Transfer Coefficient
PlaneInlet
1.624e+01
1.497e+01
1.370e+01
1.243e+01
1.116e+01
9.896e+00
8.628e+00
7.360e+00
6.091e+00
4.823e+00
3.555e+00
2.286e+00
1.018e+00
[W m^-2 K^-1]
Outlet
Inlet
Outlet
Inlet
ANSYS
R19.1
Academic
0
5.000
10.000 (m)
2.500
7.500
Y
Z
X

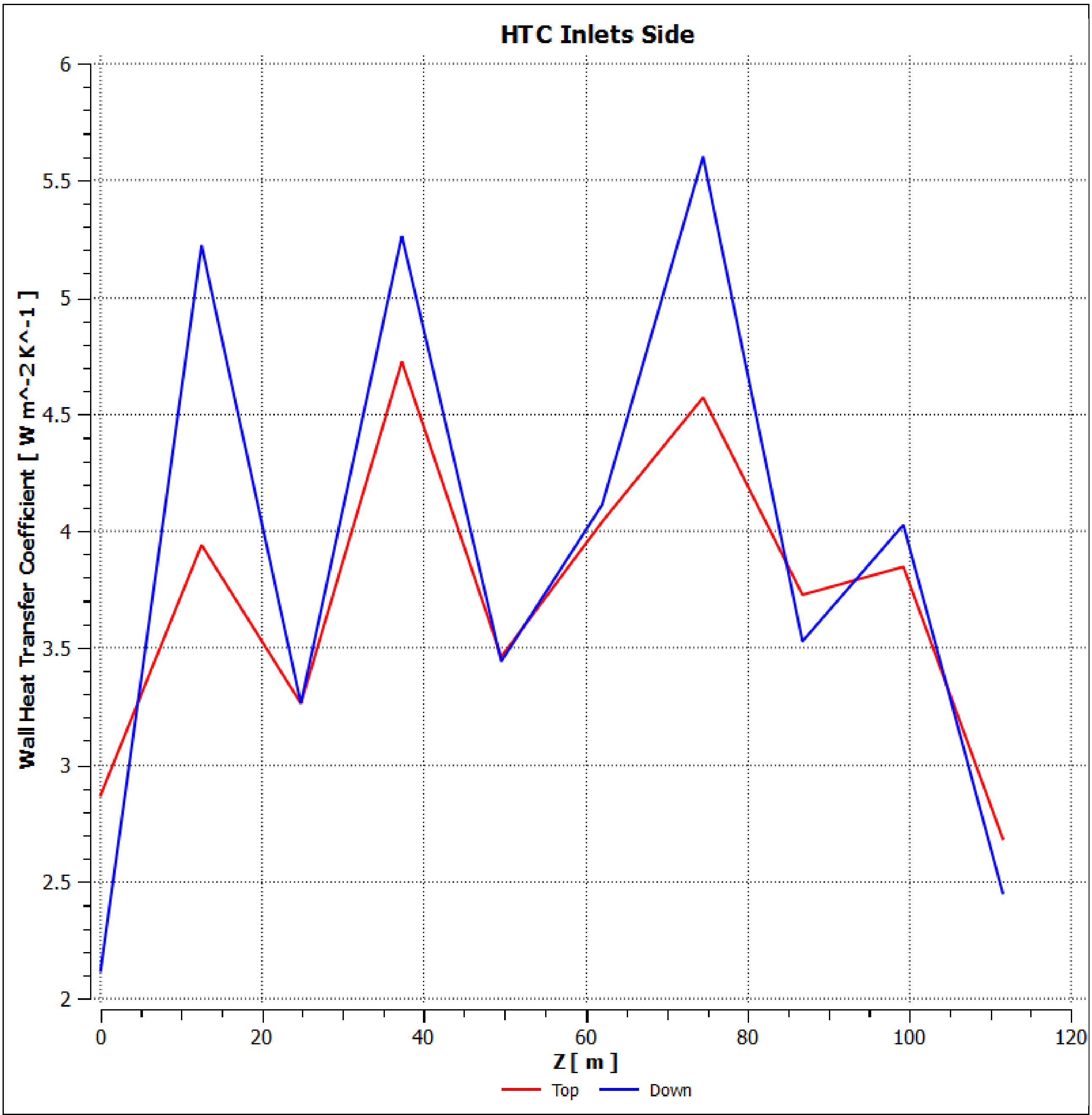
HTC Inlets Side
Wall Heat Transfer Coefficient [W m^-2 K^-1]
6
5.5
5
4.5
4
3.5
3
2.5
2
0
20
40
60
80
100
120
Z [m]
Top
Down

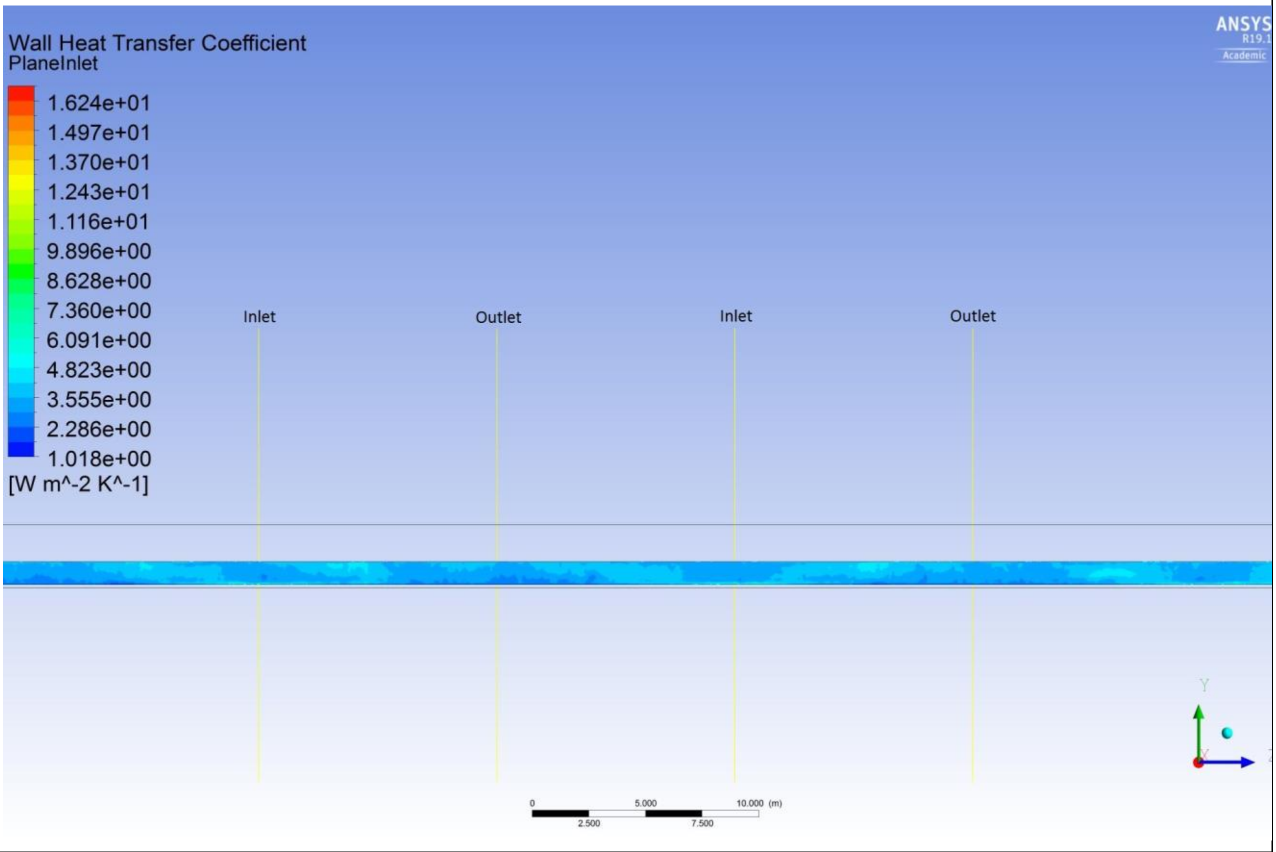
Wall Heat Transfer Coefficient
PlaneInlet
1.624e+01
1.497e+01
1.370e+01
1.243e+01
1.116e+01
9.896e+00
8.628e+00
7.360e+00
6.091e+00
4.823e+00
3.555e+00
2.286e+00
1.018e+00
[W m^-2 K^-1]
Inlet
Outlet
Inlet
Outlet
ANSYS
R19.1
Academic
0
5.000
10.000 (m)
2.500
7.500

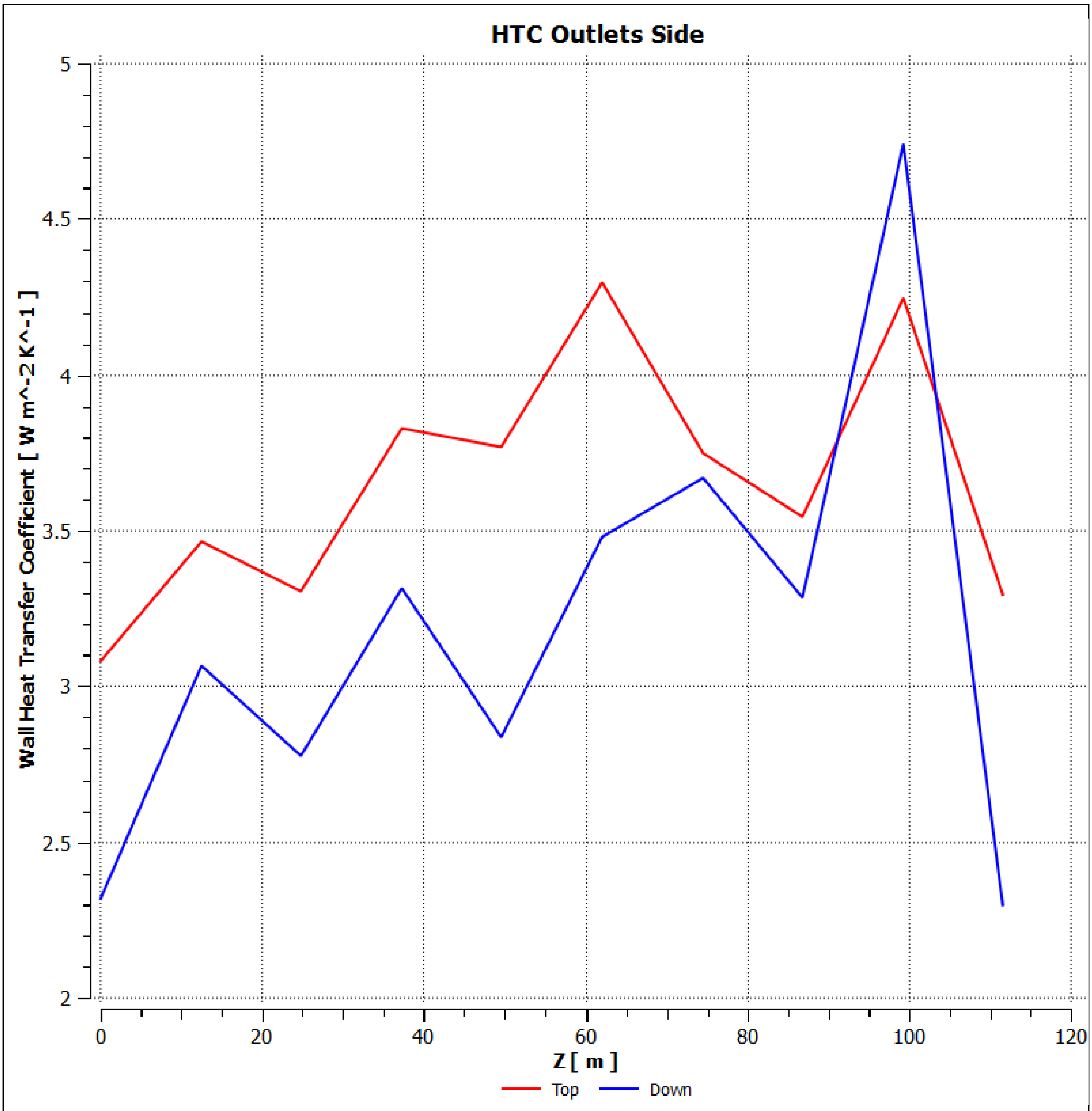
HTC Outlets Side
Wall Heat Transfer Coefficient [W m^-2 K^-1]
5
4.5
4
3.5
3
2.5
2
0
20
40
60
80
100
120
Z [m]
Top
Down

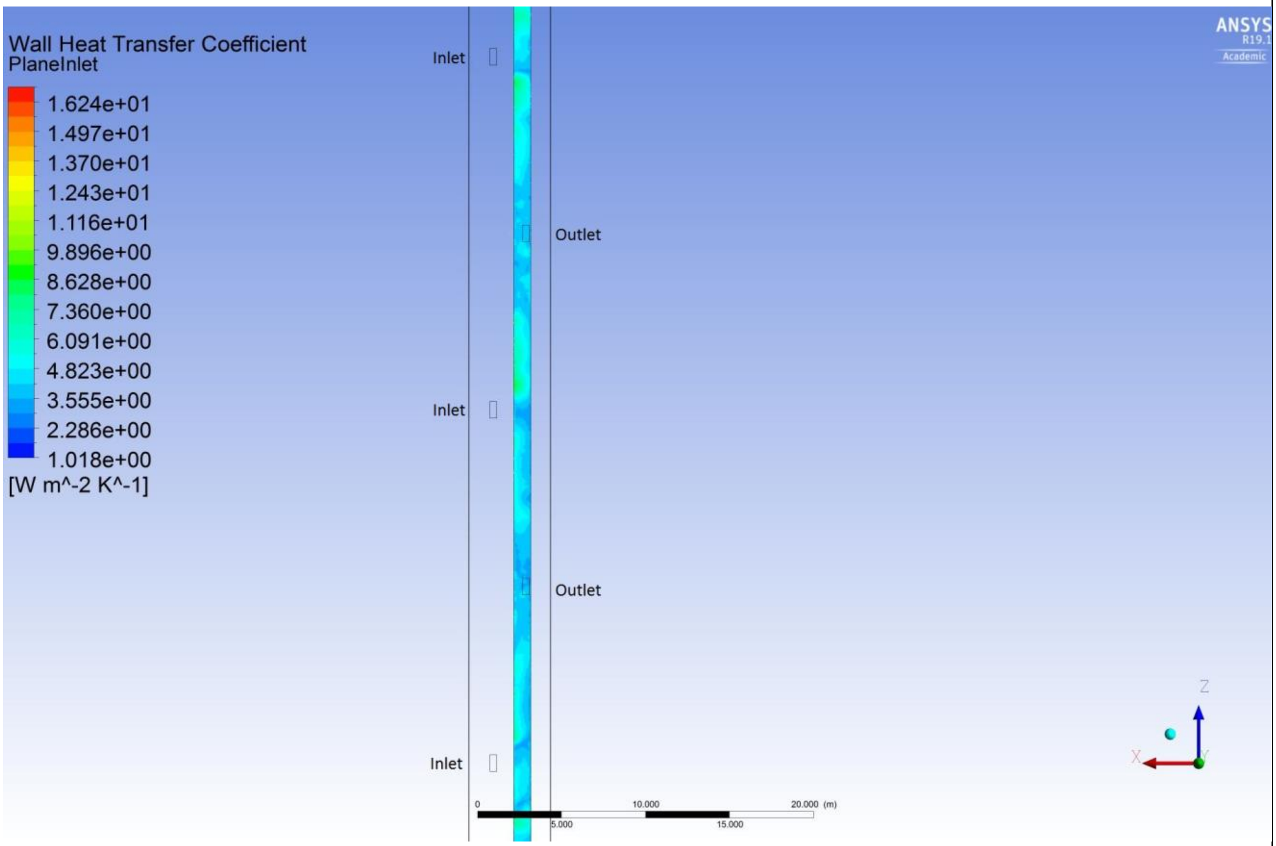
Wall Heat Transfer Coefficient
PlaneInlet
1.624e+01
1.497e+01
1.370e+01
1.243e+01
1.116e+01
9.896e+00
8.628e+00
7.360e+00
6.091e+00
4.823e+00
3.555e+00
2.286e+00
1.018e+00
[W m^-2 K^-1]
Inlet
Outlet
Inlet
Outlet
Inlet
0
5.000
10.000
15.000
20.000 (m)
ANSYS
R19.1
Academic
Z
X

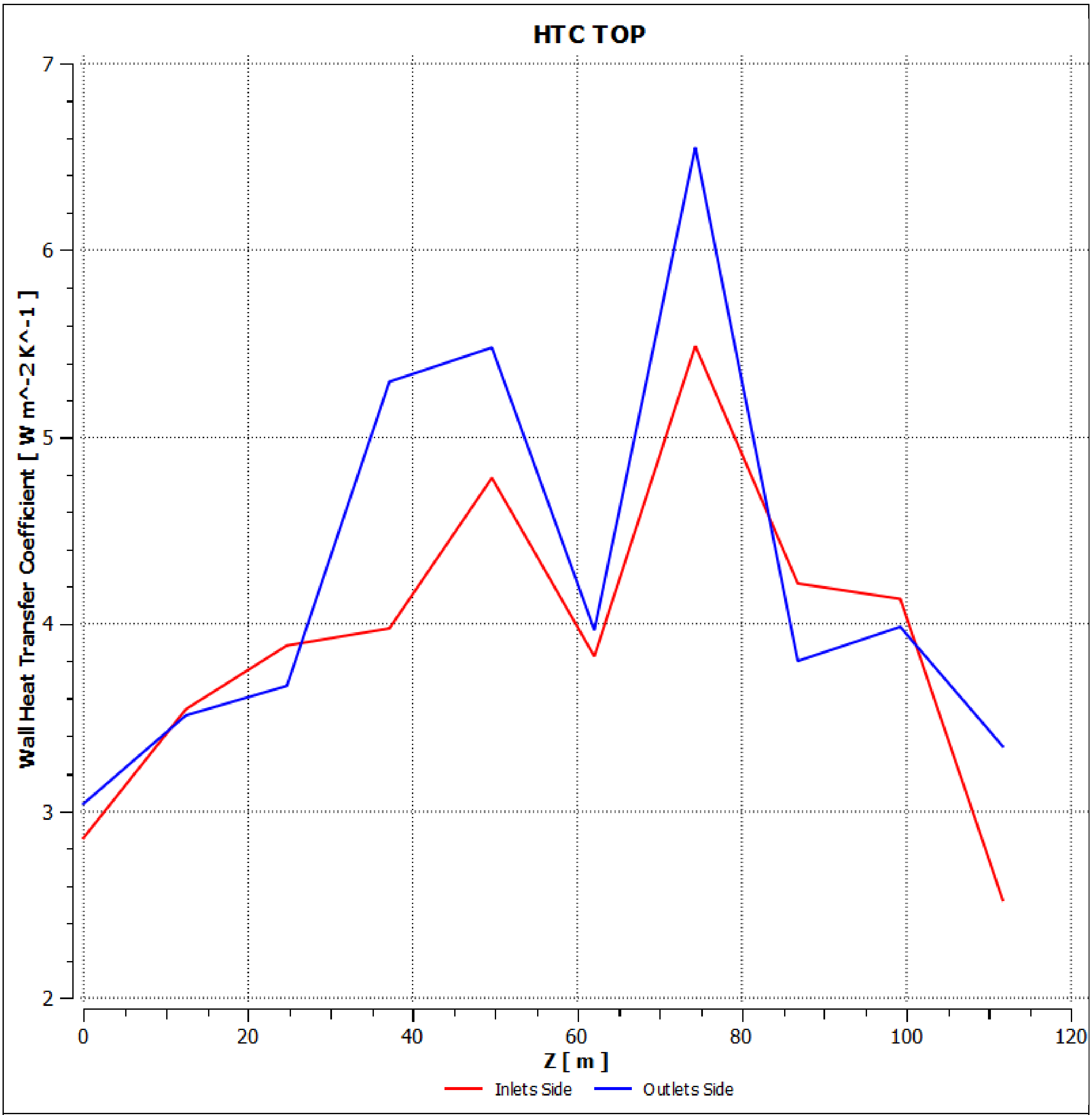

9. CONCLUSIONS

1. The temperature distribution in the tunnel does not become less irregular when the inlets and outlets are inverted.
2. The inversion of the grilles does not seem to be a good solution to enhance the temperature distribution.